Original Research Article

Compression of images of dermatological manifestations of paucisymptomatic COVID-19 patients through periodic principal components

Wilmar Hernandez.[1*] Orcid. https://orcid.org/0000-0003-4643-8377
Alfredo Mendez.[2] Orcid. https://orcid.org/0000-0002-9732-2131
Urbano Solis Cartas.[3] Orcid. http://orcid.org/0000-0003-0350-6333
Jorge Luis Valdés González.[4] Orcid. http://orcid.org/0000-0002-2661-8517
Fabricio Marcillo.[5] Orcid. https://orcid.org/0000-0003-2628-9167

[1]Ph.D. in Electronic Engineering, Universidad de las Américas, Ecuador.
[2]Ph. D. in Mathematics, Universidad Politécnica de Madrid, Madrid, Spain.
[3]Rheumatology Specialist, Universidad Nacional de Chimborazo, Escuela Superior Politécnica de Chimborazo, Riobamba, Chimborazo, Ecuador.
[4]Dermatology Specialist, Escuela Superior Politécnica de Chimborazo, Ecuador.
[5]Systems and Informatics Engineer, University of Granada, Granada, Spain.
Departamento de Investigación. Instituto Superior Tecnológico Japón. Quito, Ecuador.

[*]**Corresponding author:** Email: wilmar.hernandez@udla.edu.ec

ABSTRACT

Introduction: The management of medical images has been gaining followers based on the advantages it offers for the diagnosis of diseases, which, like COVID-19, present with clinical manifestations that can be captured in the form of images.

Objective: Take advantage of the quasi-periodicity of the principal components (PCs) in the decomposition into PCs of medical images, which represent dermatological manifestations in paucisymptomatic patients of COVID-19.

Methodology: Here, a set of photos was taken of one of the most frequent patterns in COVID-19, the maculopapular pattern, characterized by an erythmatopapular rash, and compression of one of the medical images was performed. Said compression was carried out in different ways: (1) using two PCs, (2) using both a periodic PC and a non-periodic PC, (3) using two periodic PCs, (4) using a single PC, and (5) using a single periodic PC.

Result: The results of this research proved that it is possible to work with acceptable reconstructions of compressed images in the field of dermatology, without losing the quality and characteristics that allow to reach a correct diagnosis. In addition, this achievement permits to correctly classify many diseases without fear of being wrong.

Conclusion: With the method presented, the use of a robust medical image compression technique that could be very useful in the field of health is proposed. The images allow the diagnosis of diseases such as COVID-19 in paucisymptomatic patients, understanding them allows minimizing their weight without losing quality, which facilitates their use and storage.

Keywords: principal components, principal components modified by periodicity, image reconstruction, images of dermatological diseases, maculopapular pattern.

Recibido: 05/12/2022

Aceptado: 18/12/2022

Introduction

COVID-19 is a viral disease with many clinical manifestations, among which dermatological manifestations attract attention because of its high incidence of occurrence.[1-5] In addition, sometimes signs and symptoms of COVID-19 are dermatological manifestations in patients without respiratory manifestations.[6,7] Therefore, at this time of pandemic, it is extremely important for medicine and especially for the specialty of dermatology to have images that allow the diagnosis of diseases.[8–11]

Nowadays, the acquisition and processing of medical images constitutes a very important research area. In addition, the reconstruction of medical images has found many applications.[8, 12] Furthermore, other applications involving image reconstruction are also found in industrial electronics,[13–16] and in machine vision.[17]

At present, doctors share large volumes of images, many of which are taken and saved for diagnosis. Therefore, doctors need robust technologies for image interpretation and analysis that avoid losses in quality and features, and that facilitate behavioral patterns identification of the human organism that are manifestations of possible contagion of diseases. To do this, medical images need large amounts of bits to be stored, specifically the ones with high

resolution. In addition, for their right transmission networks cannot have limited bandwidth. Therefore, the high bandwidth consumption and the growing demand for huge information storage, make it necessary to count on procedures that allow an efficient low bitrate compression of medical images. In this way, it is intended to carry out the fast, efficient transmission of these images.

What was mentioned in the previous paragraph implies carrying out a compression process. In short, the amount of data must be reduced to represent the images of interest under study, eliminating data that do not provide relevant information on the content of those images. Moreover, while the losses due to the degradation of the image are tolerable, what is lost is insignificant compared to what is gained due to the decrease in file size. Thus, the losses due to the degradation of the image are compensated with what is gained by reducing the size of the files that contain them.

In this paper, the Principal Component Analysis (PCA) technique,[18–30] is used to carry out the reduction in the dimension of medical images that represent dermatological manifestations in paucisymptomatic patients of COVID-19. The main objective of this paper is to apply PCA to the compression of a set of photos taken of one of the most frequent patterns in COVID-19, the maculopapular or morbilliform pattern, which is characterized by an erythmatopapular rash. The rationale behind this research is to try to use lossy compression techniques in medical imaging with a view to solve the problem that it is very difficult to study compressed medical images to diagnose a disease. The proposal is to provide means for the reconstruction of medical images in such a way that we do not lose significant qualities or characteristics of the disease, helping doctors to interpret and improve the diagnosis. This also the motivation of this paper.

The objective of this paper is to present a new application of the PCA technique in the field of industrial electronics, aimed at compressing of medical images. In this case, the quasi-periodicity of the first principal components (PCs),[26-28,29] is used to perform medical image compression. In short, PCs that are considered periodic are replaced by their period plus a trend, and the reconstruction achieved allows to diagnose some skin diseases.

Methodology

For the study, we have a set of 20 images of paucisymptomaticv COVID-19 patients, with different resolutions and of different parts of their bodies, where dermatological manifestations are shown. Fig. 1 shows a collage of the images under study. In order to

obtain reasonable reconstructions of compressed images, they were compressed using the PCA technique.

Figure 1. A set of images of patients with paucisymptomatic dermatological manifestations of COVID-19

At this point, it is important to mention that to obtain the images, the first thing that was done was to have the authorized consent of each patient, to take the photographs and publish them for scientific research purposes. The photos were taken with the Huawei P30 Lite MAR-LX3A smartphone along with the Magnifier Camera 1.6.0 for Android application. Here, to take the photos, the most recent lesions that are illustrative of the maculopapular pattern were chosen and with good lighting, at a reasonable distance between 50 mm and 105 mm, the photos were taken.

In this paper, from the set of images under study (see Fig. 1), one with good resolution and for which the size in pixels was divisible by 8, both in rows and in columns, was chosen. Furthermore, this image was a representative of a maculopapular pattern. Fig. 2 shows the chosen image, its resolution is 720×12800, and in the rest of the paper it will be called Img. Once the color images are obtained, they are converted from the RGB to YUV color model. This model defines 3 components: 1 luminance and 2 chrominance. Therefore, now each

image consists of 3 arrays of equal dimensions. And the aforementioned image (i.e., Img) has three components: Img1, Img2, and Img3. Each of these three matrices is divided into non-overlapping 8×8 matrices, and each of the blocks formed by those submatrices forms a vector of dimension 64.

Figure 2. Representative image of a maculopapular pattern.

Next, for the luminance matrix (i.e., the Img1 matrix) a matrix of blocks of dimension 144000×64 is formed, which we will call X1 and in which each row represents the vectors previously formed. Likewise, this process is repeated for the two chrominance matrices (i.e., Img2 and Img3), forming the X2 and X3 matrices for the Img2 and Img3 matrices respectively. So now, for each image we will have three block matrices, and to each of these matrices we apply the method of principal components with periodicity.[26-28,29]

After analyzing the decomposition of Img for each of the matrices Img1, Img2 and Img3, in order to decide the number of PCs to choose, we first analyze the growth of explained variability. In this sense, the number of PCs to take into account would be the one that exceeds a certain threshold. We worked with a threshold equal to 90%. Knowing the number of PCs, we will know the compression rate, CR. Specifically, if to compress lossless we need 64 PCs, and we compress m PCs, then the compression rate will be given by (eq:1).

$$CR=(64-m)/64 \quad \text{(eq:1)}$$

Another aspect to consider is to check the quality of the compression to know if the process is efficient. To measure the quality of the compression, we will use the peak signal-to-noise ratio (PSNR) coefficient,[26,29] which compares the differences between the compressed image and the original image to verify the quality. We will also calculate the mean square error (MSE) of the differences between the original and compressed images.[26,29]

Finally, it will be a doctor who would give the go-ahead to find out if the compressions performed meet the expected expectations. In this case, the dermatology specialists who are members of the work team will confirm that the reconstructions of the compressed medical images can be used to diagnose and classify the disease.

Results and discussions

To apply the method described in section methodology, the image under study (i.e., Img) is divided into blocks and decomposed into PCs. Fig. 3 shows the first largest eigenvalues and the explained variability by selecting those eigenvalues for the first matrix of Img (i.e., Img1) with its matrix of blocks X1. We carried out this analysis for the three matrices of Img, and built the X2 and X3 block matrices as well. These block matrices turned out to be analogous, in the sense that the first eigenvalue is very large (99.1427) compared to the second (0.5270). Furthermore, the growth of the explained variability stabilized from two principal components. Moreover, with the first two PCs, more than 99.6% of the variability shown by the matrix of the image blocks is obtained (see Fig. 3(b)).

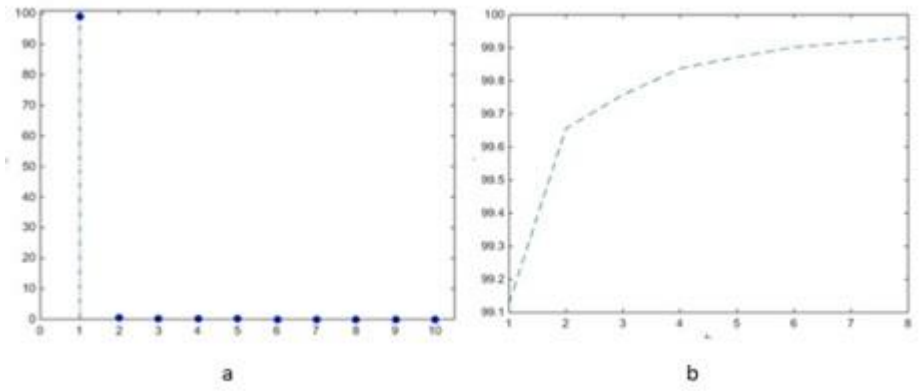

Figure 3. Magnitude of the first eigenvalues and explained accumulated variance
(a) Magnitude (λ_k) of the first 10 eigenvalues $(k, k = 1 \dots 10)$
(b) Cumulative variability (I_k) explained with the first 8 eigenvalues $(k, k = 1 \dots 8)$.

PSNR and MSE of the original image versus the compressed images are then calculated, as PCs are added to the compression. Fig. 4 shows these coefficients for the selected image (i.e., Img). In addition, this figure shows that from the first principal component the PSNR is greater than 30 and that this value grows, of course, until it reaches 100, which is the value obtained by considering all the principal components. This figure also shows a very strong drop in the value of the MSE, when taking the first 10 principal components. After this value, the MSE gradually falls to 0. The two graphs shown in Fig. 4 allow selecting the number of principal components with criteria based on the quality of the compression.

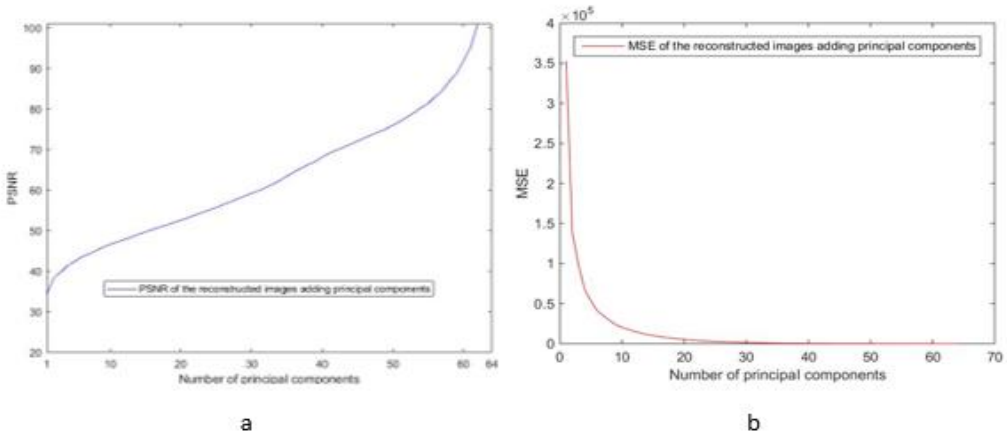

Figure 4. PSNR and MSE of the original image versus the compressed images as PCs are added to the compression.
(a) PSNR of the original image versus the compressed images;
(b) MSE of the original image versus the compressed images.

On the other hand, the compression rate (see (1)) decreases linearly as more principal components are used for compression. Fig. 5 shows the evolution of the compression rate as more principal components are added.

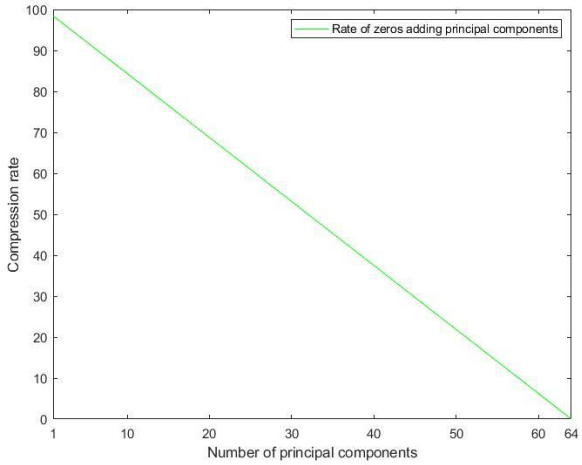

Figure 5. Compression rate of the original image as principal components are added

In view of the obtained results, we decided to compress with one and two CPs. By compressing the Img image with two CPs, an explained variability of 99.6%, a PSNR of 38.2797, and a compression rate of 96.8% are obtained. While when compressing the same image with only one CP, the explained variability drops to 99.1%, the PSNR also drops to 34.2335 and the compression rate rises to 98.4%. Fig. 6 shows the result of the compressions.

a b c

Figure 6. Original image compressed by using one and two PCs.
(a) Original image: A maculopapular pattern; (b) Original image compressed by using two PCs; (c) Original image compressed by using one PC

When saving the compressed images in .jpg format, the size of the original image is 45060 bytes and that of the compression with two CPs is 24274 bytes, this being 53.9% of the size of the original image. Regarding the compression with one CP, the size of this is 22561 bytes, being 50.1% of the size of the original image.

Next, we verify that, effectively, when making the graphs of the first PCs, they present periodic characteristics. Fig. 7 shows the graphs of the first three PCs of X1. As can be seen, the values of the first PC are almost all the same, ranging from 0.1242 to 0.1258. So, they almost form a horizontal line. Thus, we compute the 8 median values with lag 8, generate a vector of period 8 and size 64, and substitute it into the first principal component. We do this for each of the three matrices X1, X2 and X3.

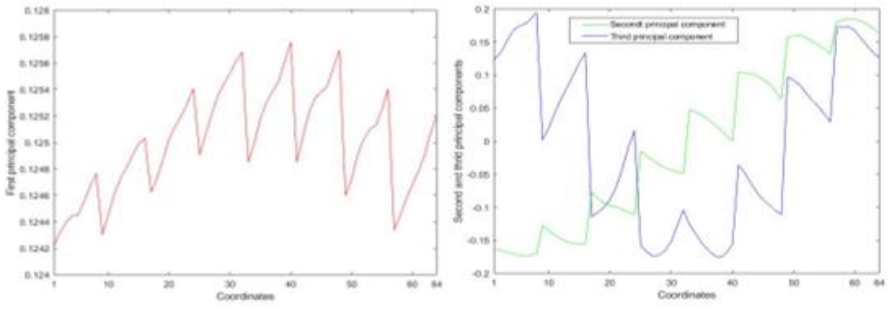

a b

Figure 7. Graphs of the first three PCs of X_1.
(a) First PC; (b) Second and third PCs.

In Fig. 7(b), the second PC shows a linear trend. After removing that trend, we take the residuals, recalculate the median of the values with lag 8, generate a vector of period 8 of dimension 64, and add the previously removed trend to this vector.

Fig. 8(a) shows the compression of the original image with only one periodic PC. In this case, the PSNR is 24.0421 and the compression rate is 99.8%. In this case, since the PSNR is less than 30, the compression has a low quality. This is noted because this reconstructed medical image is virtually devoid of sufficient color to show manifestations of dermatological disease.

On the other hand, the compressed image with two PCs, the first of these being the one that was replaced by periodicity, is shown in Fig. 8(b). This image has a PSNR value of 38.2492 and its compression rate is 98.2%. Furthermore, the compressed image with two periodic PCs is shown in Fig. 8(c). The PSNR of this image is 33.7260 and the compression rate is 99.6%.

The compressed image in .jpg format with a periodic PC has a size of 19677 bytes, which is 43.7% of the size of the original image. The image compressed with two PCs, the first PC being periodic, has a size of 21240 bytes, being 47.1% of the original image size. And, for compression with two periodic PCs, the size of this image is 20642 bytes, which is 45.8% of the original image size.

Figure 8. Different compressions of the original image, with one and two PCs, and using the periodicity of the first PCs
(a) One periodic PC; (b) Two PCs, with the first periodic; (c) Two PCs, with both periodic.

After explaining the principal component and periodic principal component methods applied to the medical image that represents a maculopapular pattern, Table I presents a summary of the characteristics of the compressions performed.

Table 1. Characteristics of compressed images

Compression	Explained cumulative variability	PSNR	Compression rate (%)	Image size reduction (%)
One PC	99.1	34.2335	98.4	49.9
Two PCs	99.6	38.2797	96.8	46.1
One Periodic PC		24.0421	99.8	56.3
Two PCs, with the first periodic		38.2492	98.2	52.9
Two PCs, with both periodic		33.7260	99.6	54.2

From the point of view of dermatology, the doctors that were consulted expressed that in all the photos one of the most frequent patterns in COVID-19, the maculopapular or morbilliform pattern, can be observed with very good sharpness and clarity. This pattern is clinically manifest in the patient shown in Fig. 2 and is characterized by a widespread erythmatopapular rash on the lower back. This rash extends to the right buttock in almost its entirety. In addition, in the medical images shown, both in the original and in the reconstructed ones, erythematous papules can be seen, some of the normal color of the skin, small, a few millimeters long, some of them raised and others not. Also, it is observed that these papules converge, leaving areas of healthy skin inside. All this allows to reach the diagnosis of the pathology without any difficulty, both in the original photo and in those that are compressed. As discussed in this section, the lowest quality image is the compression with one periodic principal component, but even this image conveys relevant information.

Conclusions

This paper has presented a compression method for medical images that represent dermatological manifestations in paucisymptomatic patients with COVID-19. Specifically, a representative image of the maculopapular pattern was chosen, and different types of compression were performed on it, guaranteeing the validity of the compressed images to diagnose the disease. The presented method is based on principal component analysis and on the quasi-periodicity of the first principal components, in the case of medical images of patients. Good compression ratios were achieved here, while maintaining quality and relevant features. At this time of pandemic, this is of the utmost importance in the field of medicine and even more so in the specialty of dermatology, because in this, images are a fundamental pillar in the diagnosis of diseases. Therefore, being able to work with lower-weight images without losing the characteristics of the original image allows a correct diagnosis to be made and many diseases to be classified without fear of making mistakes.

Finally, it can be concluded that, with the method presented in this paper, the authors propose the use of a robust medical-image compression technique that could be very useful in the field of dermatology.

Acknowledgments

The authors would like to express their gratitude and respect to their colleague Alfredo Mendez at the Universidad Politécnica de Madrid, Spain. After helping them write the initial draft of this paper, Alfredo Mendez passed away in September 2022. His help, passion, and inspiration made not only this research, but many another research works possible. This research was supported in part by the Universidad de Las Américas (UDLA), Quito, Ecuador, under Research Project IEA.WHP.21.01, and in part by the Corporación Ecuatoriana para el Desarrollo de la Investigación y la Academia (CEDIA), Ecuador, under Research Project CEPRA XVI-2022-02-IMAGENES COVID.

Bibliographic reference

1. Madigan LM, Micheletti RG, Shinkai K. How Dermatologists Can Learn and Contribute at the Leading Edge of the COVID-19 Global Pandemic. JAMA Dermatol. [Internet]. 2020 [citado 2022 Nov 16];156(7):733-4. Disponible en: https://pubmed.ncbi.nlm.nih.gov/32352485/
2. Diaz-Guimaraens B, Dominguez-Santas M, Suarez-Valle A, Pindado-Ortega C, Selda-Enriquez G, Bea-Ardebol S, et al. Petechial Skin Rash Associated With Severe Acute Respiratory Syndrome Coronavirus 2 Infection. JAMA Dermatol. [Internet]. 2020 [citado 2022 Nov 14];156(7):820-2. Disponible en: https://jamanetwork.com/journals/jamadermatology/fullarticle/2765614
3. Recalcati S. Cutaneous manifestations in COVID-19: a first perspective. J Eur Acad Dermatol Venereol. [Internet]. 2020 [citado 2022 Nov 13];34(5):e212-3. Disponible en: https://pubmed.ncbi.nlm.nih.gov/32215952/
4. Tammaro A, Adebanjo GAR, Parisella FR, Pezzuto A, Rello J. Cutaneous manifestations in COVID-19: the experiences of Barcelona and Rome. J Eur Acad Dermatol Venereol. [Internet]. 2020 [citado 2022 Nov 16];34(7):e306-e7. Disponible en: https://pubmed.ncbi.nlm.nih.gov/32330340/

5. Campanati A, Brisigotti V, Diotallevi F, D'Agostino GM, Paolinelli M, Radi G, et al. Active implications for dermatologists in 'SARS-CoV-2 ERA': Personal experience and review of literature. J Eur Acad Dermatol Venereol, [Internet]. 2020 [citado 2022 Nov 15];34(8):1626-32. Disponible en: https://pubmed.ncbi.nlm.nih.gov/32426855/
6. Johnson KD, Harris C, Cain JK, Hummer C, Goyal H, Perisetti A. Pulmonary and Extra-Pulmonary Clinical Manifestations of COVID-19. Front Med, [Internet]. 2020 [citado 2022 Nov 12];7:526. Disponible en: https://www.ncbi.nlm.nih.gov/pmc/articles/PMC7438449/
7. Chih-Cheng L, Wen-Chien K, Ping-Ing L, Shio-Shin J, Po-Ren H. Extra-respiratory manifestations of COVID-19. Int J Antimicrob Agents, [Internet]. 2020 [citado 2022 Nov 16];56(2):106024. Disponible en: https://www.sciencedirect.com/science/article/pii/S0924857920301874
8. Ye B, Yuan X, Cai Z, Lan T. Severity Assessment of COVID-19 Based on Feature Extraction and V-Descriptors. IEEE Transactions on Industrial Informatics, [Internet]. 2021 [citado 2022 Nov 13];17(11):7456-67. Disponible en: https://ieeexplore.ieee.org/document/9346008
9. Park GH, Song YA, Choi HJ. Compression Algorithms for Imaging Instruments - A Mini Review. Journal of Multidisciplinary Engineering Science and Technology (JMEST), [Internet]. 2022 [citado 2022 Nov 15];9(1):14923-9. Disponible en: https://www.jmest.org/vol-9-issue-1-january-2022/
10. Devaraj SJ. Emerging Paradigms in Transform-Based Medical Image Compression for Telemedicine Environment. En: Hemanth DJ, Balas, EM, editors. Telemedicine Technologies. Academic Press [Internet]. 2019 [citado 2022 Nov 18];2(3):15-29. Disponible en: https://www.sciencedirect.com/science/article/pii/B9780128169483000027
11. Aloupogianni E, Ishikawa M, Kobayashi N, Obi T. Hyperspectral and multispectral image processing for gross-level tumor detection in skin lesions: a systematic review. J Biomed Opt, [Internet]. 2022 [citado 2022 Nov 14];27(6):060901. Disponible en: https://pubmed.ncbi.nlm.nih.gov/35676751/
12. Lo FP, Sun Y, Qiu J, Lo BPL. Point 2 Volume: A Vision-Based Dietary Assessment Approach Using View Synthesis. IEEE Transactions on Industrial Informatics, [Internet]. 2020 [citado 2022 Nov 13];16(1):577-86. Disponible en: https://ieeexplore.ieee.org/document/8853329

13. Halim MSA, Hadi NA, Sulaiman H, Abd Halim S. An algorithm for beta-spline surface reconstruction from multi slice CT scan images using MATLAB pmode. Proceedings of the 2017 IEEE Symposium on Computer Applications and Industrial Electronics (ISCAIE) [Internet]. 2017 [citado 2022 Nov 14];23(38):24-5. Disponible en: https://ieeexplore.ieee.org/document/8074939
14. Ronagh M, Eshghi M. Hybrid Genetic Algorithm and Particle Swarm Optimization Based Microwave Tomography for Breast Cancer Detection. Proceedings of the 2019 IEEE 9th Symposium on Computer Applications and Industrial Electronics (ISCAIE); 2019 Apr 27-28; Kota Kinabalu, Malaysia. IEEE. Disponible en: https://ieeexplore.ieee.org/document/8743814
15. Tan SL, Mat Som MH, Basaruddin KS, Sulaiman AR, Aziz Safar MJ, Amin Megat Ali MS. Finite Element Analysis on Tibia with Osteogenesis Imperfecta: The Influence of Incomplete Bone in Model Reconstruction. Proceedings of the 2020 IEEE Symposium on Industrial Electronics and Applications (ISIEA); 2020; TBD, Malaysia. IEEE. Disponible en: https://ieeexplore.ieee.org/document/9188155
16. Miao Y, Wang S, Miao Y, An M, Wang X. Stereo-based Terrain Parameters Estimation for Lower Limb Exoskeleton. Proceedings of the 2021 IEEE 16th Conference on Industrial Electronics and Applications (ICIEA); 202; Chengdu, China. IEEE. Disponible en: https://ieeexplore.ieee.org/document/9516267
17. Sonka ML, Hlavac V, Boyle R. Image Processing, Analysis, and Machine Vision. 4th ed. Cengage Learning; 2015. Disponible en: https://www.thefreelibrary.com/Image+Processing%2C+Analysis%2C+and+Machine+Vision%2C+4th+Edition.-a0392254098
18. Jackson JE. User's Guide to Principal Components. John Wiley & Sons; 1991. Disponible en: https://www.wiley.com/en-us/A+User%27s+Guide+to+Principal+Components-p-9780471471349
19. Diamantaras KI, Kung SY. Principal Component Neural Networks: Theory and Applications. John Wiley & Sons; 1996. Disponible en: https://www.wiley.com/en-us/Principal+Component+Neural+Networks%3A+Theory+and+Applications-p-9780471054368
20. Elsner JB, Tsonis AA. Singular Spectrum Analysis: A New Tool in Time Series Analysis. Plenum Press; 1996. Disponible en: https://www.amazon.com/Singular-Spectrum-Analysis-Language-Science/dp/0306454726

21. Rencher, AC. Multivariate Statistical Inference and Applications, 1st ed. Wiley-Interscience; 1997. Disponible en: https://www.wiley.com/en-us/Multivariate+Statistical+Inference+and+Applications-p-9780471571513
22. Flury B. First Course in Multivariate Statistics. Springer-Verlag; 1997. Disponible en: https://link.springer.com/book/10.1007/978-1-4757-2765-4
23. Gnanadesikan R. Methods for Statistical Data Analysis of Multivariate Observations, 2nd ed. Wiley-Interscience; 1997. Disponible en: https://www.wiley.com/en-us/Methods+for+Statistical+Data+Analysis+of+Multivariate+Observations,+2nd+Edition-p-9780471161196
24. Jolliffe IT. Principal Component Analysis. Springer; 2002. Disponible en: https://link.springer.com/book/10.1007/b98835
25. Wichern DW, Johnson RA. Applied Multivariate Statistical Analysis. 6th ed. Pearson; 2007. Disponible en: https://www.amazon.com/Applied-Multivariate-Statistical-Analysis-6th/dp/0131877151
26. Hernandez W, Mendez A. Application of Principal Component Analysis to Image Compression. En: Türkmen Göksel. STATISTICS. Rijeka: InTechOpen; 2018:107-37. Disponible en: https://www.intechopen.com/chapters/59936
27. Hernandez W, Mendez A, Ballesteros F. Image Noise Cancellation by Taking Advantage of the Principal Component Analysis Technique. En: Proceedings of the 44th Annual Conference of the IEEE Industrial Electronics Society - IECON 2018; 2018; Washington, DC, USA. IEEE. Disponible en: https://ieeexplore.ieee.org/document/8591437
28. Hernandez W, Mendez A, Quezada-Sarmiento PA, Jumbo-Flores LA, Mercorelli P, Tyrsa V, et al. Image compression based on periodic principal components. En: Proceedings of the IECON 2019- 45th Annual Conference of the IEEE Industrial Electronics Society; 2019; Lisbon, Portugal. IEEE. Disponible en: https://ieeexplore.ieee.org/document/8926747
29. Hernandez W, Mendez A. Image Compression Technique Based on Some Principal Components Periodicity. En: Sergiyenko, O, Rivas-Lopez, M, Flores-Fuentes, W, Rodríguez-Quiñonez, JC, Lindner, L. Control and Signal Processing Applications for Mobile and Aerial Robotic Systems. Hershey, PA: IGI Global; 2020:309-27. Disponible en: https://www.igi-global.com/chapter/image-compression-technique-based-on-some-principal-components-periodicity/243770

30. Abdi H, Williams LJ. Principal component analysis. WIREs Computational Statistics. 2010;2(4):433-59. Disponible en: https://wires.onlinelibrary.wiley.com/doi/abs/10.1002/wics.101

Conflicts of interest

The authors do not report conflicts of interest

Authors contribution

Wilmar Hernandez: He participated in the conception of the research, information search, study methodology, writing and final review of the manuscript.

Alfredo Mendez: He participated in the conception of the research, information search, study methodology, writing and final review of the manuscript.

Urbano Solis Cartas: He participated in the search for information and writing of the manuscript.

Jorge Luis Valdés González: He participated in the search for information and writing of the manuscript.

Fabricio Marcillo: He participated in the search for information and writing of the manuscript.